*Microscopy and Microanalysis*, **31** (7), 2025, 1998–2003
https://doi.org/10.1093/mam/ozaf048.999

Microscopy AND Microanalysis

**Proceedings**

# Comparison and Evaluation of the Corrosion Behavior of Two Innovative $B_4C$ Samples Doped with 0.5% and 3% FeNiCoCrMo High-Entropy Alloy

**Alberto Daniel Rico-Cano[1], Julia Claudia Mirza-Rosca[1,2,*], Burak Cagri Ocak[3], and Gultekin Goller[3]**

[1]*Department of Mechanical Engineering, University of Las Palmas de Gran Canaria, Las Palmas de Gran Canaria, Spain.*
[2]*Materials Engineering and Welding Department, Transilvania University of Brasov, Brasov, Romania*
[3]*Department of Metallurgical and Materials Engineering, Istanbul Technical University, Istanbul, Turkey*

*Corresponding author: julia.mirza@ulpgc.es

Boron carbide ($B_4C$) is widely recognized for its exceptional hardness (30 GPa), elevated melting point (2450°C), low density (2.52 g/cm$^3$), neutron absorption capacity (600 barns), high corrosion resistance and thermal stability and conductivity (30 W/m K) [1, 2]. All these attributes make it an ideal candidate for a large range of engineering applications like armor, nuclear shielding, ballistic or refractory industry [3].

High-entropy alloys (HEAs) have emerged as promising reinforcement materials due to their unique mechanical and electrochemical properties, such as enhanced strength, corrosion resistance, and phase stability [4]. These materials consist of multiple principal elements in near-equiatomic proportions [5, 6]. The union of HEAs and ceramic materials, like $B_4C$, has shown potential for improving on structural, mechanical and corrosion properties [7, 8]. In particular, FeNiCoCrMo HEA-reinforced $B_4C$ composites resulted to improved exhibit enhanced corrosion resistance due to the formation of stable passive layers [9, 10].

Thus, the purpose of the present study is to compare and evaluate, using different electrochemical tests, the influence of FeNiCoCrMo high-entropy alloy reinforcement on the corrosion behaviour of $B_4C$ ceramic, in a simulated aggressive environment, 3.5% NaCl solution. Furthermore, a statistical analysis of the microhardness results will provide insight into the mechanical performance of the synthesized materials.

The new materials used in this research, object of comparison, are 2 boron carbide matrix composites doped with 0.5% and 3% of FeNiCoCrMo HEA, created at Istanbul Technical University by Spark Plasma Sintering technic (SPS-7.40 MK-VII, SPS Syntex Inc.). For the corrosion and microhardness tests conducted, the composites ingots were embedded in a two-component epoxy resin, after a day, the resin dries and the samples can be easily handle for the tests. Afterwards, the samples were polished using the Struers TegraPol-11 polisher with progressive silicon carbide papers from 250 to 2000 grit and finally to achieve a mirror-like finish, 0.1 µm alpha alumina suspension polishing cloths were used (see Fig. 1).

The embedded samples were subjected to electrochemical and microhardness testing. Three electrochemical tests were conducted, using a potensiostat (BioLogic Essential SP-150), in order to determine their chemical behavior: corrosion potential, corrosion rate and Electrochemical Impedance Spectroscopy. These tests were carried out on a simulated marine environment, a 3.5% in volume NaCl solution. The materials Vickers microhardness was then measured by using a FM-810 Microhardness Tester (Future Tech). Indentations were carefully spaced to prevent interference in the measurements. Due to the material hardness, a load of 2 kgf was applied to guarantee accurate measurements and clearly defined indentations marks. The test was conducted in accordance with the ISO 14577-1:2015 standard [11]. At least, a total of 45 indentations were performed on different regions of each of the samples. The average Vickers hardness ($HV_2$) values were then calculated and the statistical analysis executed to compare the mechanical performance of both compositions.

The electrochemical tests conducted on both samples revealed clear results about their corrosion behaviour. As shown in Fig. 2., the sample with 3% HEA has a more noble (less negative) and stable corrosion potential, increasing from the initial stages of immersion till 4 hours, which implies the creation of a protective passive film, indicating greater corrosion resistance. In contrast, the 0.5% HEA sample corrosion potential was defined by a significant drop during the first 12 hours of immersion, indicating corrosion was attacking the composite. For the following 12 hours its corrosion potential remained stable, suggesting even though it has higher susceptibility to degradation and lower stability in the saline environment than the 3% HEA sample, 0,5% HEA composite finally passivated. Polarization curves show that the 3% HEA sample has a lower corrosion current density, implying a reduced electrochemical degradation rate. On the other hand, the 0.5% HEA sample exhibits a higher anodic current, indicating higher corrosion of the material.

The electrochemical impedance spectroscopy provided clear insight into the electrochemical behavior of $B_4C$ doped with 0.5% and 3% HEA in marine environment, see Fig. 3. The 3% HEA-doped sample exhibits a higher impedance in the Nyquist curve (60.047 kΩ) than the 0.5% HEA-doped B4C (4.241 kΩ), indicating better corrosion resistance. For both samples, R(Q(R(QR)Q(RW))), the equivalent circuit model is the same, which implies distinct resistive and capacitive contributions. The presence of Warburg element indicates diffusion processes, suggesting that the corrosion mechanism involves ion transport limitations. The Warburg element has a bigger presence in the 3% HEA sample, indicating the formation of a more stable passive layer, corroborating the other electrochemical test results. The Bode impedance plot further supports the improved corrosion resistance of the 3% HEA sample, while the phase angle plot reveals differences in charge transfer mechanisms. These findings suggest that higher HEA content enhances the protective behavior of the composite.

The microhardness statistical analysis, shown in Fig. 4, was performed through various plots (boxplots, histograms and normal distribution), generated to visualize and compare the hardness behavior of both samples. The $B_4C$ 3% HEA sample exhibits a higher median hardness compared to the $B_4C$ 0.5% HEA sample, alongside a narrower distribution of values, indicating improved homogeneity.

Research on the B4C doped composites gives more information about the chemical and mechanical behaviour of these new materials. The electrochemical tests remarked that the 3% HEA B4C sample presented the highest corrosion resistance, suggesting that a higher HEA content enhances the protective behavior of the composite. In the statistical microhardness analysis, the tests conducted clearly show that 3% HEA $B_4C$ composite have higher hardness and even though both follow a normal distribution, 3% HEA $B_4C$ presented a more homogeneous structure. These results suggest that the increase of HEA in $B_4C$ is related to improvements in both mechanical and chemical behaviour. However, future research lines could explore other concentrations (e.g., 1%, 2%, 4% or higher) to identify optimal composition and analyze the underlying trends more comprehensively.

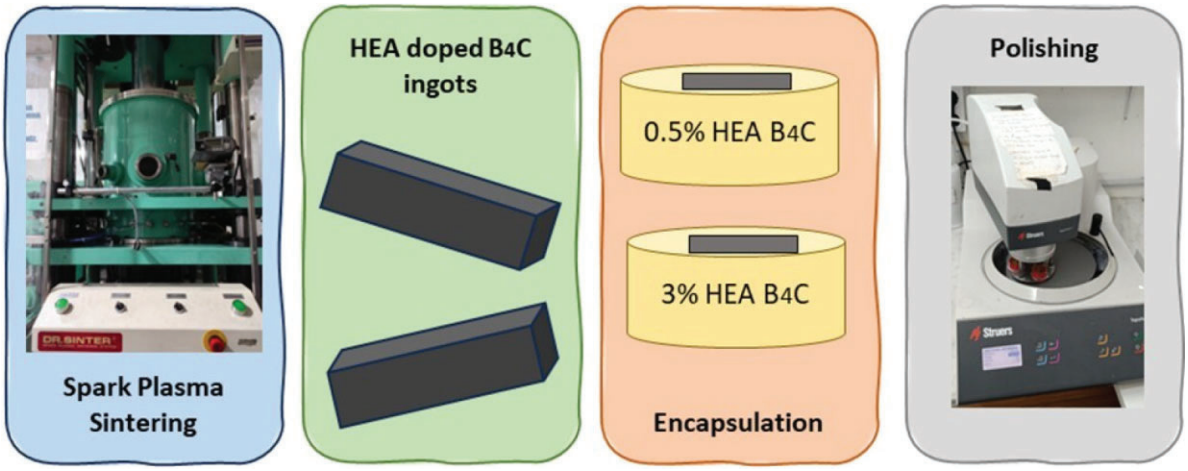


**Fig. 1.** Fabrication and preparation of the $B_4C$ samples under study.

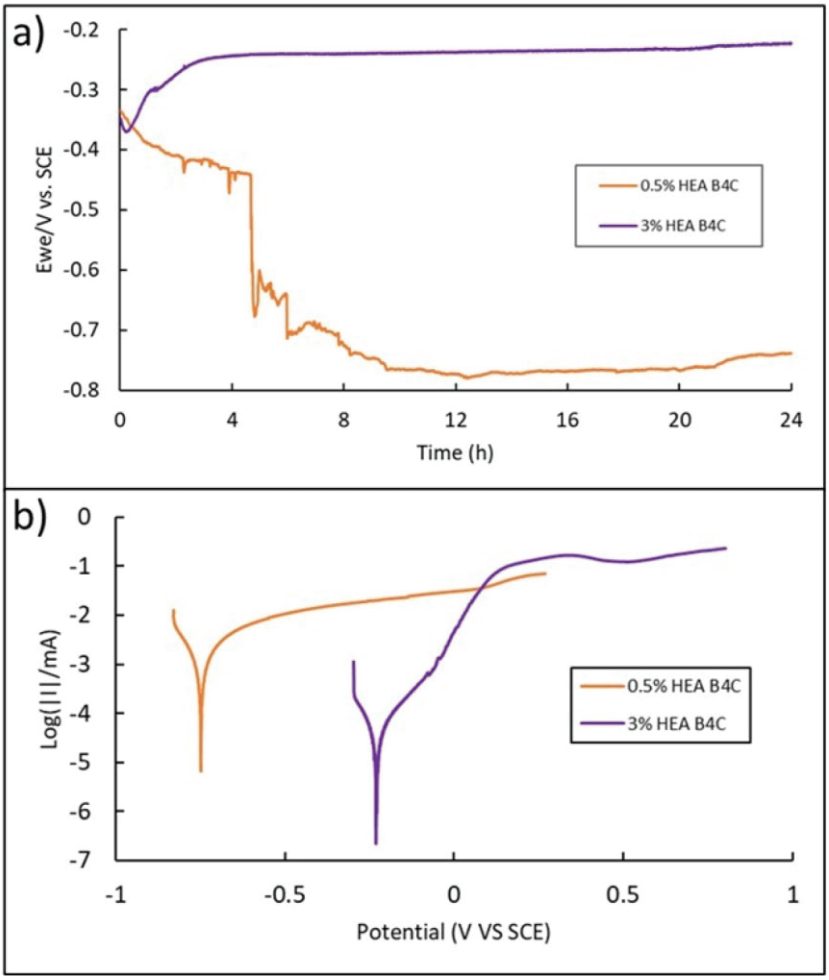


**Fig. 2.** Corrosion potential vs. time for 24 h of immersion (a)), corrosion rate (b)), for both $B_4C$ HEA-doped samples in 3.5% NaCl solution.

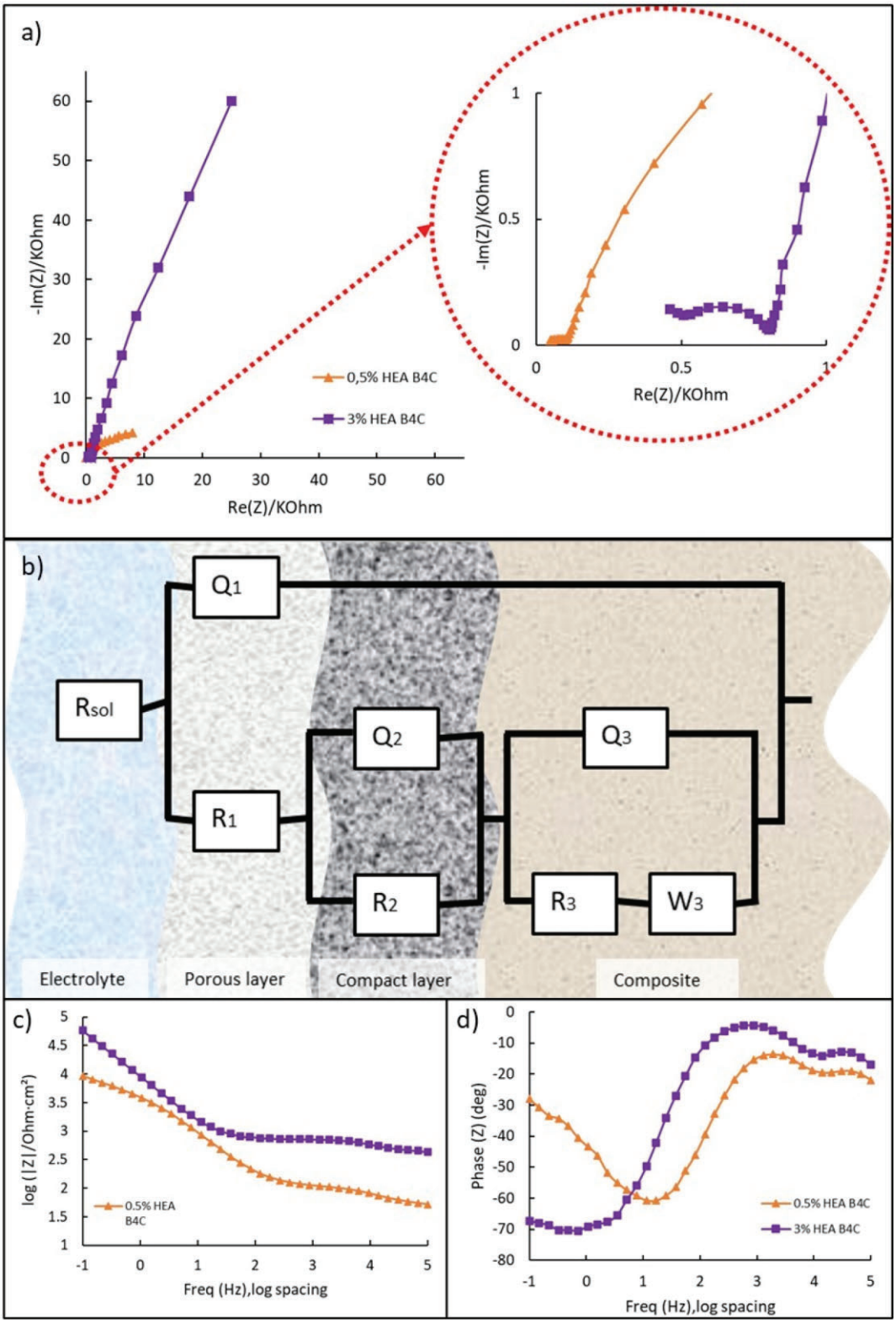


**Fig. 3.** Nyquist diagram (a)), equivalent electrical circuit applied (b)), Bode impedance diagram (c)), Bode phase diagram (d)), for doped samples at Ecorr after 24 h of immersion in 3.5% NaCl solution.

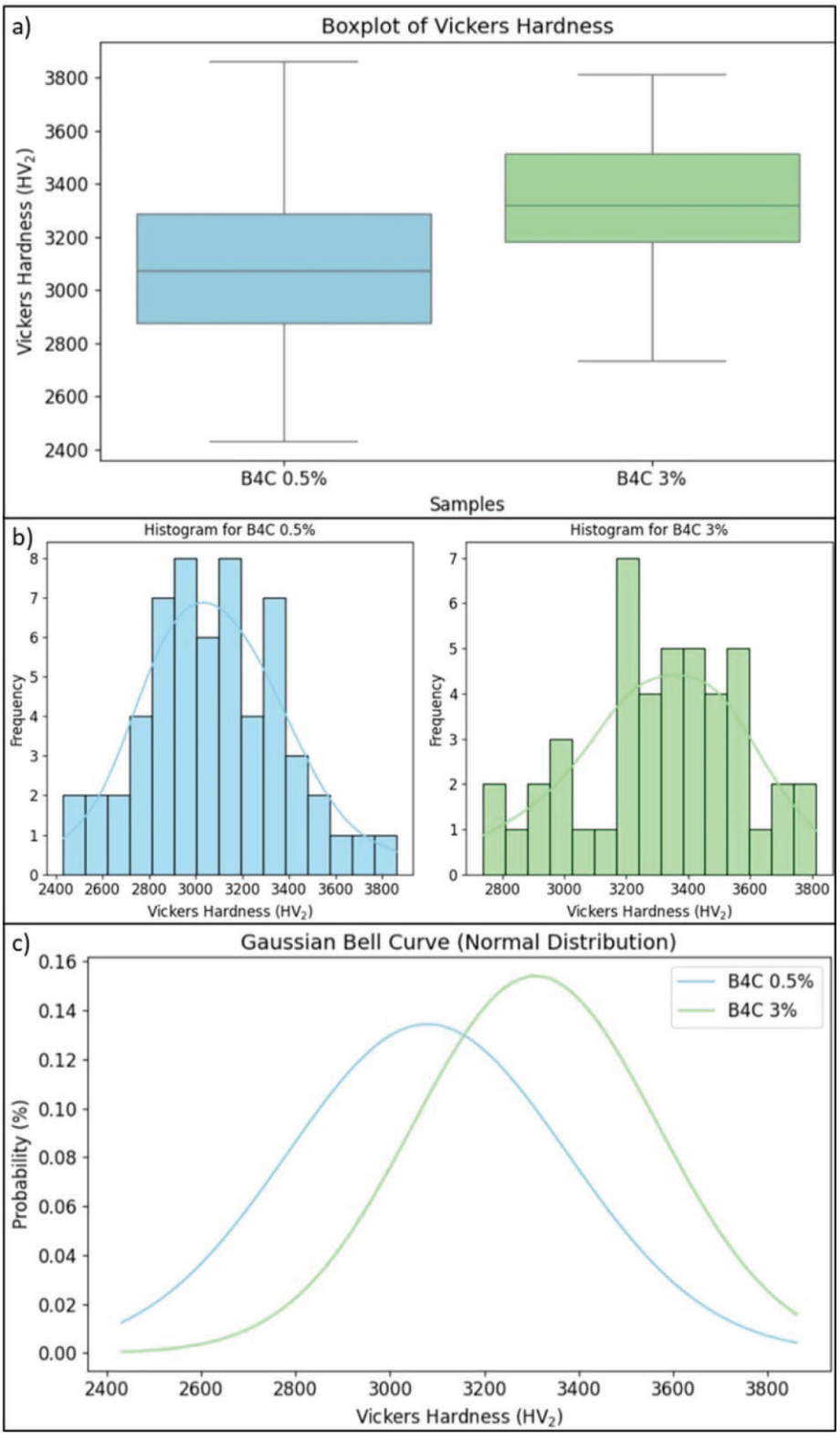


**Fig. 4.** Distribution of Vickers hardness data through its quartiles (a), frequency of Vickers hardness values within certain intervals (bins) (b)) probability distribution of the hardness values (c)), comparison for $B_4C$ doped samples.

## References

1. Suri AK *et al. International Materials Reviews* (2010) 55 4–38. https://doi.org/10.1179/095066009X12506721665211
2. Pérez S *et al. Progress in Nuclear Energy* (2024) 175 https://doi.org/10.1016/j.pnucene.2024.105320

3. Domnich V *et al. Journal of the American Ceramic Society* (2011) **94** 3605–3628. https://doi.org/10.1111/j.1551-2916.2011.04865.x
4. Cui G *et al. Journal of Materials Research and Technology* (2020) **9** 2598–2609. https://doi.org/10.1016/j.jmrt.2019.12.090
5. Chen J *et al. Journal of Alloys and Compounds* (2018) **760** 15–30. https://doi.org/10.1016/j.jallcom.2018.05.067
6. Miracle DB and Senkov ON. *Acta Mater* (2017) **122** 448–511. https://doi.org/10.1016/j.actamat.2016.08.081
7. Ahn SY *et al. Journal of Alloys and Compounds* (2023) **960**. https://doi.org/10.1016/j.jallcom.2023.170631
8. Gul AO *et al. Intermetallics* (2022) **146**. https://doi.org/10.1016/j.intermet.2022.107593
9. Rico-Cano AD *et al. Metals* (2025) **15** 79. https://doi.org/10.3390/met15010079
10. Rico-Cano AD *et al. Microscopy and Microanalysis* (2024) **30** https://doi.org/10.1093/mam/ozae044.666
11. ISO 14577-1:2015 Metallic Materials—Instrumented Indentation Test for Hardness and Materials Parameters—Part 1: Test Method n.d. ISO: Geneva, Switzerland 2015.